

## Research on the Traceability Method of Adhesive Resistance Strain Gauge Values

Yu Wu<sup>1</sup>, Dengke Gan<sup>1,\*</sup>, Rui Xue<sup>2</sup>, Yanfei Ren<sup>2</sup>, Ping Wu<sup>2</sup>

<sup>1</sup>Chongqing Academy of Metrology and Quality Inspection, Chongqing, China

<sup>2</sup>Chongqing Airport Group CO., LTD., Chongqing, China

\*Corresponding Author

**Abstract:** This article establishes a mathematical measurement model for calibrating adhesive resistance strain gauges based on the definition of strain values. Through experimental research, the influence of tensile coaxiality on strain measurement results was analyzed, and two different eccentric forms of tensile morphology were discovered in the experiment. A metal flat strip tensile morphology monitoring method based on three-point angle monitoring method was proposed. In addition, combined with finite element numerical simulation, the influence of lateral force on the measurement results was studied. The results showed that when the axial load was loaded to 10%, there was an approximately linear relationship between the axial strain of the metal strip and the tensile load. The research results provide theoretical basis and technical support for strain gauge calibration and optimization of testing methods.

**Keywords:** Strain Gauges; Traceability of Measurement Values; Coaxiality; Lateral Force

### 1. Introduction

Strain testing technology is widely used in aerospace, chemical, metallurgical industries, civil engineering, materials engineering, and other fields.<sup>[1~4]</sup> It is a common means of testing, analyzing, and evaluating the reliability and safety of structural design, manufacturing, and assembly. The methods of strain measurement can be divided into two categories: strain electrical measurement method and strain optical measurement method. The strain gauge electrical measurement method is a testing system composed of strain gauges, resistance strain gauges, and related instruments attached to the tested object. All machinery or

components will undergo a certain degree of deformation when subjected to load. This relative displacement causes a relative change in the resistance, capacitance, or inductance of the strain gauges, which are then connected to the strain gauge. The strain measurement value is finally obtained through the measurement circuit and amplifier of the strain gauge. Among them, the measurement accuracy of the sensitivity coefficient of strain gauges directly affects the accuracy of actual strain measurement. At present, there is a calibration regulation JJG 623-2005 for resistance strain gauges in China, and the optimal static strain gauge accuracy level has reached 0.1. However, without obtaining calibrated sensitivity coefficients of strain gauges, it is difficult to ensure that the measurement results obtained by the entire measurement system also have such high accuracy. Therefore, it is crucial to calibrate the sensitivity coefficient of the corresponding transformer (meter) in this situation.<sup>[5~7]</sup>



**Figure 1. Adhesive Resistance Strain Gauge**

### 2. Research on Traceability Method of Strain Value

This article starts from the definition of strain value and designs a loading device for uniaxial tension of metal flat bars. By measuring the displacement tension of the middle measuring section of the metal flat bar, the theoretical strain value is calculated using the strain definition formula. At the same time, the strain

gauge is attached to the middle section of the metal strip, and the strain measurement error of the strain gauge is obtained by comparing the theoretical strain value with the measured strain gauge reading. The stress state of the displacement measurement section in the axial tension of a metal strip can be considered as a uniaxial stress state that conforms to the assumption of a flat section. The strain value measurement model is shown in Equation 1:

$$\varepsilon = \frac{\Delta L}{L} \quad (1)$$

$\varepsilon$  is the calculated strain value,  $\Delta L$  is the relative displacement change at both ends of the known span after the experiment, in units of  $\mu\text{m}$ , and  $L$  is the known span labeled for a single experiment, in units of  $\mu\text{m}$ .

The closed-loop control force source of the strain gauge calibration device is considered to use a force standard machine, which has a relatively high overall stiffness compared to the tested sample and is not prone to deformation. The force standard machine is installed on a stable foundation as a whole, and the standard force gauge is connected in series with the tested sample through corresponding fixtures, connectors, or reverse frames. The set force value is mechanically applied to the metal plate (sample) to produce elastic deformation (small displacement). The control of the screw rotation is driven by a servo motor. In the axial direction of stretching and compression, when the control screw pair stops the knob, the screw pair engages with the screw, and the screw stops rotating, the automatic locking of the crossbeam can be achieved.

For measuring  $L$  in mathematical models, using end face standards of various specifications such as gauge blocks, it is characterized in the measurement section of a metal flat bar. Then, using a specially designed hanging platform, the top pin on the platform is accurately positioned on the engraved line. By using physical measuring tools, the distance between the optical mirror groups for linear measurement is determined.

For measuring  $\Delta L$  in the mathematical model<sup>[8]</sup>, we choose to use the principle of laser interference to accurately install optical spectrometers and interferometers at both ends of the labeled known span, and use the difference in the paths of the two beams of light

to obtain the deformation of the metal strip.

### 3. Analysis of Influence Variables in Strain Calibration Test

#### 3.1 The Influence of Coaxiality on Measurement Results During Strain Stretching Process

Considering the impact of the misalignment between the centerline of the upper and lower pull head components and the centerline of the strain standard plate on the strain standard quantity, a three-point corner monitoring method is designed in this experiment. Measurement process: Install the strain standard plate on the upper and lower pull head components, sequentially install the hanging plate and optical measuring mirror group (angle reflector) on the three sections of the strain standard plate, middle and lower, and install the hanging plate and optical measuring mirror group (angle interferometer) on fixed points, or sequentially install the hanging plate and optical measuring mirror group (angle reflector and angle interferometer) on the strain standard plate, middle, middle and lower sections. Through this measurement method, the relative rotation angle of the strain standard plate between detection point 1 (upper section), detection point 2 (middle section), and detection point 3 (lower section) is detected.

According to the force analysis, under the tensile load of the lower pull head components in this project, the strain standard plate will produce two basic characteristic tensile forms. The first type is a tensile form that is eccentric in both upward and downward directions. There is an eccentricity in the same direction between the center line of the joint bearings in the upper and lower tension components and the upper and lower tension holes on the strain standard plate. The calculation formula is shown in Equation 2

$$\varepsilon_{add} = \frac{\tan \frac{\varphi}{2}}{l} \quad (2)$$

The second type is the tensile form with different eccentricities in the upper and lower directions. There are eccentricities in different directions between the strain standard plate's upper and lower extension holes and the centerline of the joint bearings in the upper and lower tensile components. Because the upper and lower extension holes of the strain standard

plate are located in opposite directions to the joint bearings in the upper and lower tension components, and because it is an antisymmetric structure, the pin shafts in the upper and lower tension components will cause relative angular displacement  $\varphi$  in the upper and lower extension holes of the strain standard plate. At this time, this form can be decomposed into an equal cross-section single span statically indeterminate beam with two fixed ends. The two statically indeterminate beams are antisymmetric loads, with one end of each beam having no angular displacement and the other end having angular displacement  $\varphi$ . According to structural mechanics, for any statically indeterminate beam, the bending moment load at the angular displacement end is  $\frac{4EI}{l}$ , and the bending moment load at the end

without angular displacement is  $\frac{2EI}{l}$ . Through linear superposition, the loads at both ends of the strain standard plate are  $\frac{6EI}{l}$ ,  $\frac{6EI}{l}$

Experimental research: Using the principle of laser interference to measure the half amplitude angular characteristics of symmetric or antisymmetric structures of the sample under the condition of an upper and lower eccentricity of 100mm, as well as under the condition of an upper and lower eccentricity of 100mm.

**Table 1. Measurement Results of Relative Rotation Angle of Cross Section under Eccentric Tensile Configuration in the Upper and Lower Directions**

| section (°)     | 1#-2#Relative angle of cross-section | 2#-3#Relative angle of cross-section |
|-----------------|--------------------------------------|--------------------------------------|
| Tensile load(N) |                                      |                                      |
| 500             | 0.0                                  | 0.0                                  |
| 1000            | 90.9                                 | 134.4                                |
| 1500            | 138.4                                | 236.1                                |
| 2000            | 173.6                                | 316.4                                |
| 3000            | 225.9                                | 438.4                                |
| 5000            | 285.9                                | 600.3                                |
| 7000            | 323.9                                | 712.6                                |
| 9000            | 355.2                                | 803.3                                |

**Table 2. Measurement Results of Relative Rotation Angle of Cross-Sections under Different Eccentric Tensile Shapes in the Upper and Lower Directions**

| section (°)     | 1#-2#Relative angle of cross-section | 2#-3#Relative angle of cross-section |
|-----------------|--------------------------------------|--------------------------------------|
| Tensile load(N) |                                      |                                      |
| 500             | 0                                    | 0                                    |
| 1000            | 47.9                                 | 58.9                                 |
| 1500            | 76.8                                 | 114.1                                |
| 2000            | 104.0                                | 159.0                                |
| 3000            | 144.6                                | 232.9                                |
| 5000            | 187.3                                | 334.8                                |
| 7000            | 211.5                                | 401.2                                |
| 9000            | 222.5                                | 451.6                                |

| section (°)     | 3#-4#Relative angle of cross-section | 4#-5#Relative angle of cross-section |
|-----------------|--------------------------------------|--------------------------------------|
| Tensile load(N) |                                      |                                      |
| 500             | 0                                    | 0                                    |
| 1000            | 36.2                                 | 25.5                                 |
| 1500            | 54.5                                 | 42.0                                 |
| 2000            | 63.3                                 | 56.1                                 |
| 3000            | 81.1                                 | 65.5                                 |
| 5000            | 89.1                                 | 85.6                                 |
| 7000            | 86.0                                 | 91.5                                 |
| 9000            | 77.1                                 | 94.2                                 |

From the measurement results obtained from actual experiments, it is relatively easy to distinguish the characteristics of eccentric tensile shapes in different directions up and down, as well as eccentric tensile shapes in the same direction up and down.

### 3.2 The Influence of Lateral Force on Measurement Results During Strain Stretching Process

Considering the bending problem of thin plates caused by the lateral force of hanging plates and linear measuring mirror groups, in elasticity, if the thickness of the plate is much smaller than the minimum size of the middle surface, this plate is called a thin plate because the thickness of the metal strip is much smaller than the minimum size of the middle surface, which can actually be regarded as a thin plate. When a thin plate is subjected to a general load, the load can be divided into two sub loads. One is a longitudinal load parallel to the median plane, and the other is a transverse load perpendicular to the median plane. The axial tensile force applied to both ends of the metal strip by this device is the longitudinal load, which can be considered as uniformly distributed along the thickness direction of the thin plate. Therefore, the stress, deformation, and displacement caused can be calculated according to the plane stress problem. If the thin plate is subjected to a lateral load, it will bend, and the stress, deformation, and displacement caused by it can be calculated according to the thin plate bending problem.

The mechanical model of the metal flat bar in this device considering lateral force can be considered as a problem of small strain and large rotation. The structure undergoes large rigid body rotation, but its strain can be calculated according to the theory of linear elasticity.

The relationship between the strain matrix of the structure after a large rotation and the initial strain matrix is

$$[B_n] = [B_v][T_n]$$

$[B_v]$  is the geometric matrix in the initial coordinate system;  $[T_n]$  is the orthogonal transformation matrix between the initial coordinate system and the rotational coordinate system.

According to the principle of virtual work, the tangent stiffness matrix of the element is

$$[K_e] = \int_{vol} [T_n]^T [B_v]^T [D] [B_v] [T_n] d(vol)$$

The Newton Raphson restoring force of the unit is

$$\{F_e^{nr}\} = \int_{vol} [T_n]^T [B_v]^T [D] \{\epsilon_n^{el}\} d(vol)$$

The elastic strain is

$$\{\epsilon_n^{el}\} = [B_v] \{u_n^d\}$$

$\{u_n^d\}$  is the displacement of the element that causes strain.

In this device, due to the influence of its own gravity on the hanging plate and linear measuring mirror group, the metal flat strip exhibits thin film bending under lateral force. Under tension, a significant stress stiffening effect will occur in thin high stress structures. When the metal flat bar is gradually stretched and straightened, a gradually strengthening vertical stiffness will be generated. In order to calculate the specific bending deflection of the metal flat bar and the change process of bending deflection during the stretching process, ANSYS is used to consider this geometric nonlinear problem. The whole process is analyzed in two load steps. The first load step is the lateral force generated by the hanging plate and linear measuring mirror, which causes the metal flat bar to produce a large deflection thin plate bending. The second load step is the stretching of the metal flat bar, which gradually produces a high stress state in the thin plate. This load step considers the stress stiffness effect.

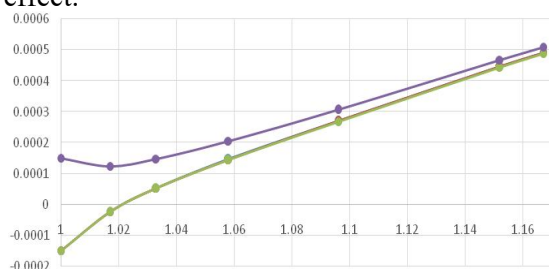


**Figure 2. Strain Finite Element Calculation Results**

It can be seen that after the axial load is loaded to 10%, the axial strain and axial tensile load

show a linear relationship. In the middle measuring section of the metal strip (within 300mm), the strain measurement values at measuring points 1 #~3 # are  $3005.32 \mu\epsilon$ ,  $3005.28 \mu\epsilon$ , and  $3005.18 \mu\epsilon$ , respectively. The fluctuation range of surface strain on one side of the metal strip measuring section is 0.005%. Due to the influence of lateral loads, metal flat bars exhibit a certain degree of deflection, but with the application of axial tensile loads, they are quickly straightened. The final strain measurement value at measuring point 4 is  $3005.51 \mu\epsilon$ , and the difference in strain between the front and rear sides of the metal strip at the same cross-sectional height is 0.006%.

#### 4. Conclusion

Starting from the definition of strain values, this article presents a mathematical measurement model for calibrating adhesive resistance strain gauges. Through experimental research, the influence of tensile coaxiality on measurement results during strain stretching was studied. It was found that there were two different eccentric forms of stretching in the experiment, and a three-point angle monitoring method was designed to monitor the stretching form of metal flat bars. In addition, the influence of lateral force on the measurement results during the strain stretching process was analyzed. Through finite element numerical simulation, it was concluded that the axial strain of the metal strip showed an approximately linear relationship with the axial tensile load when the axial load was loaded to 10%.

#### References

- [1] Zhang Z, Deng F, Huang Y, et al. Field validation of road roughness evaluation using in-pavement strain sensors[J]. Smart Materials & Structures, 2015, 24(11):115029.
- [2] Guo X, Liu Z, Zhou X. Bridge strain data acquisition system[J]. Electronic Measurement Technology, 2016.
- [3] Arrizabalaga O, Villatoro J, Durana G, et al. Assessment of a multi-core optical fibre interferometer for strain sensing in aerospace structures[C]//European Workshop on Structural Health Monitoring.2016.
- [4] Guo M. Optimization of strain gauge

- screening test method for spacecraft[J]. Application of Electronic Technique, 2016.
- [5] Lei Yiming. Strain transmit research and aberration analysis of electric resistance strain gauge[J]. Science technology and engineering, 2011, 11(32): 8096-8100.
- [6] Wang Linglu, Chen Kexing, Zhao Yinming. Digital Compensation Technology for Resistive Strain Sensors[J]. Measurement Techniques, 2016(zl):196-200.
- [7] Zhang Zhitong. Strain resistance transducer compensation technology[J]. Journal of north china institute of aerospace engineering, 2009, 19(1):21-24.
- [8] Yu Haili. Research on large stroke nan-positioning technology and application based on dual-frequency laser interferometer[D]. Chinese Academy of Sciences, 2011.